

Navigation for the MESSENGER Mission's First Mercury Encounter

K. E. Williams*, A. H. Taylor†, D. R. Stanbridge‡, P. J. Wolff§, B. R. Page** and B. G. Williams††
KinetX, Inc., Space Navigation and Flight Dynamics Practice (SNAFD), Simi Valley, CA, 93065

and

J. V. McAdams‡‡

The Johns Hopkins University Applied Physics Laboratory, Space Department, Laurel, MD, 20723

The Mercury Surface, Space ENvironment, GEOchemistry, and Ranging (MESSENGER) mission, led by principal investigator Sean C. Solomon of the Carnegie Institution of Washington, is the seventh mission in NASA's Discovery Program. The spacecraft was launched from Cape Canaveral Air Force Station on 3 August 2004, to begin its six-and-one-half-year interplanetary cruise to arrive in orbit about Mercury beginning in March 2011. The cruise phase includes planetary gravity-assist flybys of Earth (in August 2005), Venus (in October 2006 and June 2007), and Mercury (in January and October 2008 and September 2009). This paper describes the navigation results for the period encompassing Mercury flyby 1 and focuses on orbit determination results, navigation analyses supporting statistical trajectory-correction maneuvers, and maneuver reconstruction results. Also included are discussions of optical navigation performed before the encounter, and the determination of the gravitational potential of Mercury.

Selected Nomenclature

α_{SKI}	=	Sun "keep-in" angle or angle between Sun and normal to heat shield of MESSENGER spacecraft
AU	=	Astronomical Unit (149598000 km)
B-R, B-T	=	Components of B-Plane location along R and T axes, respectively
C_{nm}, S_{nm}	=	Spherical gravitational harmonics of degree n and order m
ΔDOR	=	Delta Differential One-way Ranging
DE405	=	Particular set of planetary ephemerides adopted by MESSENGER Mission
ΔV	=	Velocity change or delta-velocity
$\Delta V_{lateral}$	=	Component of velocity change directed nearly orthogonal to the Sun direction
ΔV_{radial}	=	Component of velocity change directed nearly parallel or anti-parallel to the Sun direction
$\Delta X, \Delta Y, \Delta Z$	=	Cartesian offset location vector in specified coordinate frame
J2000	=	Baseline epoch used for various coordinate frames (1 January 2000, at 12:00)
J_n	=	Zonal gravitational harmonic of degree n
R, S, T	=	Basis vectors or axes of B-plane coordinate frame
σ	=	Sigma or standard deviation of a Gaussian-distributed data sample
SEP, SPE	=	Sun-Earth-probe and Sun-probe-Earth angles, respectively, usually in degrees (°)
W	=	Data weight applied to data used for orbit determination

* MESSENGER Navigation Team Chief, 21 W. Easy St., Suite 108, Simi Valley, CA 93065, AIAA Member.

† SNAFD Flight Director, 21 W. Easy St., Suite 108, Simi Valley, CA 93065.

‡ SNAFD Navigation Analyst, 2141 E. Broadway, Suite 217, Tempe, AZ 85282, AIAA Member.

§ SNAFD Optical Navigation Analyst, 21 W. Easy St., Suite 108, Simi Valley, CA 93065.

** MESSENGER Lead Navigation Analyst, 2141 E. Broadway, Suite 217 Tempe, AZ 85282, AIAA Senior Member.

†† SNAFD Director, 21 W. Easy St., Suite 108, Simi Valley, CA 93065, AIAA Senior Member.

‡‡ MESSENGER Mission Design Lead Engineer, Space Department, 11100 Johns Hopkins Drive, Laurel, MD, 20723, AIAA Senior Member.

I. Introduction

THE Mercury Surface, Space ENvironment, GEochemistry, and Ranging (MESSENGER) mission is being flown as the seventh mission in NASA's Discovery Program. The MESSENGER mission is led by the principal investigator, Sean C. Solomon, of the Carnegie Institution of Washington. The Johns Hopkins University Applied Physics Laboratory (JHU/APL) designed and assembled the spacecraft and serves as the home for project management and spacecraft operations. Navigation for the spacecraft is provided by the Space Navigation and Flight Dynamics Practice of KinetX, Inc., a private corporation. Navigation for launch and interplanetary cruise makes use of radiometric tracking data from NASA's Deep Space Network (DSN) augmented by optical navigation from on-board images of planetary flybys.

After launch on 3 August 2004, the spacecraft began its six-and-one-half year interplanetary cruise¹ that will culminate with rendezvous and Mercury orbit insertion (MOI) beginning in March 2011. Figure 1 shows the mission timeline of planetary flybys and deterministic deep-space maneuvers (DSMs) from launch to nominal end of mission. The interplanetary trajectory includes an Earth gravity-assist flyby about one year after launch, followed by two Venus flybys and three Mercury flybys before MOI¹. Once in orbit, MESSENGER will perform science observations of Mercury for one Earth year. Spacecraft navigation during interplanetary cruise involves estimating the trajectory based on available tracking data and computing trajectory-correction maneuvers (TCMs) that deliver the spacecraft as close as possible to nominal target parameters at each planetary flyby². Since total fuel usage is carefully controlled to ensure mission success, the remaining trajectory is re-optimized after each large propulsive maneuver and planetary flyby to accommodate execution errors and trajectory uncertainties. The KinetX Navigation Team works closely with the Mission Design Team at JHU/APL to optimize flyby targets and to compute TCMs.

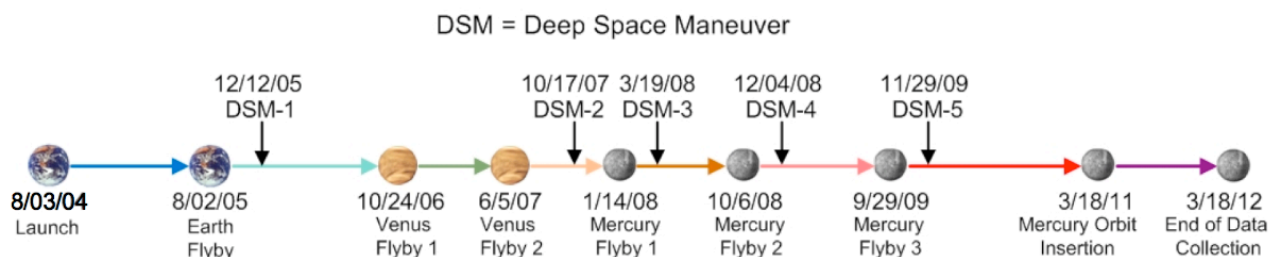


Figure 1. MESSENGER Timeline for Planetary Flybys and Deep-Space Maneuvers.

The second Venus flyby occurred on 5 June 2007, followed by Deep-Space Maneuver 2 (DSM-2) on 17 October 2007, a long solar conjunction ending around 12 December 2007, the first Mercury flyby on 14 January 2008, and Deep-Space Maneuver 3 (DSM-3) on 19 March 2008, targeting the subsequent Mercury flyby. During this period, the primary goal of the MESSENGER Navigation Team was to determine and control the spacecraft trajectory to ensure successful completion of the remainder of the cruise phase to Mercury. The spacecraft attitude was modeled and solar radiation pressure (SRP) parameters were estimated on the basis of available telemetry and DSN Doppler and ranging tracking data. The geometry of the spacecraft relative to the Sun and Earth during this period is summarized in Fig. 2.

With a closest approach altitude of approximately 200 kilometers (km), Mercury flyby 1 was more demanding than the previous Venus flyby, which had an adjusted flyby altitude of 338 km³. The flyby was complicated by trajectory uncertainties caused by a superior solar conjunction from mid-October through mid-December and trajectory correction maneuvers on either side of the conjunction. DSM-2 (also designated as TCM-18) produced a velocity change of 226 meters per second (m/s) on October 17, near the entry to the conjunction, while TCM-19 provided a small correction (1.1 m/s) to the trajectory on December 19, not long after emerging from the conjunction period. The formal definition of conjunction is when the Sun-Earth-probe angle (SEP) < 3°, and the final design for this clean-up TCM was required to be completed on the day after the exit from conjunction. This made necessary the use of tracking data with a large amount of solar-plasma-induced noise from the low SEP. This difficulty was mitigated in part by extensive use of Delta Differential One-way Ranging (Δ DOR) data⁴, first used operationally on the MESSENGER mission on the approach to Venus flyby 2. This data type once again proved extremely useful in improving the trajectory estimation on this flyby.

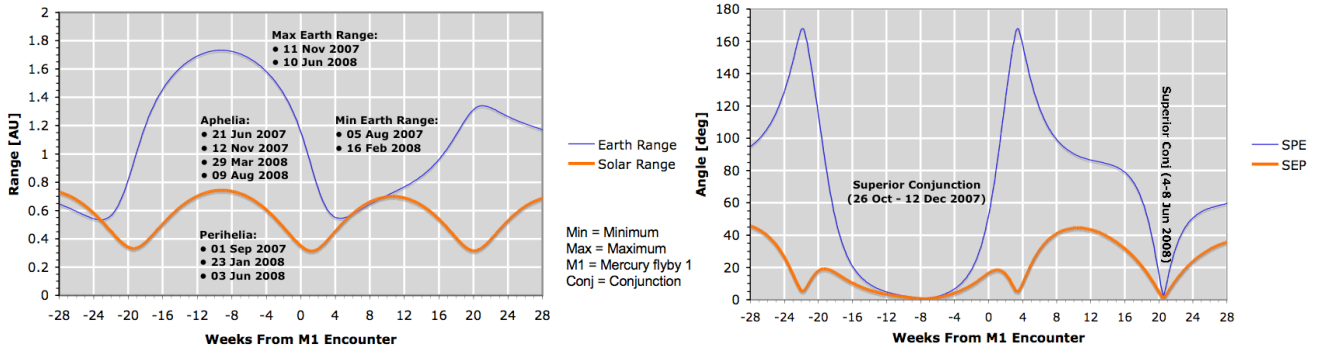


Figure 2. Sun-Earth Geometry for Period Including First Mercury Encounter.

The measure used to judge the accuracy of the estimated trajectory and trajectory correction maneuvers on approach to the flyby is the intercept point in the hyperbolic impact-plane (or B-plane) at Mercury. The B-plane is the plane normal to the incoming asymptote of the hyperbolic flyby trajectory that passes through the center of the target body (Mercury in this case). The “S-axis” is in the direction of the incoming asymptote and hence is normal to the B-plane. For MESSENGER, the “T-axis” is parallel to the line of intersection between the B-plane and the Earth Mean Orbital or Ecliptic plane of J2000 and is positive in the direction of decreasing right ascension. The “R-axis” completes the mutually orthogonal, right-handed Cartesian coordinate axes “T-R-S” and is positive toward the South Ecliptic Pole.

In addition to the superior solar conjunction, there were other challenges to navigation posed by Mercury flyby 1 and related events. Among these was the first operational use of optical navigation (OpNav) on the MESSENGER mission. OpNav was especially important since it was the only way to reveal any Mercury planetary ephemeris errors in time to plan and perform a corrective maneuver. The last close flyby of Mercury by a spacecraft had been by Mariner 10 in March 1975, so there was a possibility of significant systematic error in the location of Mercury assumed for the initial MESSENGER flyby. Such errors would not be detected early enough with Earth-based radiometric tracking alone. Another challenge revolved about the successful completion of DSMs that needed to be performed in a timely fashion to preserve fuel margin and to avoid violating Sun “keep-in” (SKI) constraints that protect vital subsystems from exposure to excessive thermal radiation. This required scheduling several contingency maneuvers in the event of an anomaly that would cause a DSM to be completely aborted or only partially completed. Subsequent to the flyby, DSM-3 also served as an initial rehearsal of the turn-while-burn mode to be employed later at MOI. All challenges to navigation raised by Mercury flyby 1 and associated events were successfully addressed, as described further in subsequent sections.

II. Navigation System Overview

The MESSENGER Navigation Team is organized as part of a multi-mission navigation support group so that the team size can be adjusted as mission events dictate. The Navigation Team was led by Tony Taylor, with Ken Williams taking over lead responsibility not long after Mercury flyby 1. The MESSENGER Navigation Team performs orbit determination (OD) and TCM reconstruction and additionally performs TCM design and trajectory re-optimization in conjunction with the Mission Design Team. OD for cruise phases is based on the following DSN radiometric data types (abbreviations shown are standard DSN designations): two-way Doppler (F2), three-way Doppler (F3), two-way ranging (SRA), and Δ DOR (IWD). Tracking of MESSENGER was obtained as described below, and verified by comparison to OD solutions predicted from previous tracking data⁴. These radiometric-only solutions are used to estimate the trajectory and certain dynamic parameters so that the predicted intercept point and its uncertainty can be used to plan TCMs that correct the trajectory back to an aimpoint within acceptable constraints and margins of error.

The MESSENGER Navigation Team is also responsible for performing OpNav. As indicated above, Mercury flyby 1 included the first operational use of OpNav on the MESSENGER mission as a means of verifying the Mercury planetary ephemeris. This capability was first tested on approach to Venus flyby 1, and was tested again following Venus flyby 2. The results of the OpNav processing for Mercury flyby 1 are discussed below.

III. MESSENGER DSN Doppler and Ranging Processing

DSN tracking coverage has been adjusted during the cruise phase to support important events such as DSMs, emergence from solar conjunctions, and the approach to Mercury flyby 1, while allowing a reduced schedule of one or two tracks per week during routine cruise intervals. The tracking schedule planned for the period surrounding Mercury flyby 1 is shown in Fig. 3. In addition to spacecraft telemetry, during a track the DSN acquires radiometric Doppler and ranging data that are passed to the Navigation Team for processing. Each coherent two-way track from a single DSN antenna produces F2 data. If a second DSN antenna receives the same downlink, such as what happens during a station-to-station handover, then F3 data are also produced. Almost every track for MESSENGER is also configured to acquire two-way ranging data from the DSN Sequential Ranging Assembly (SRA).

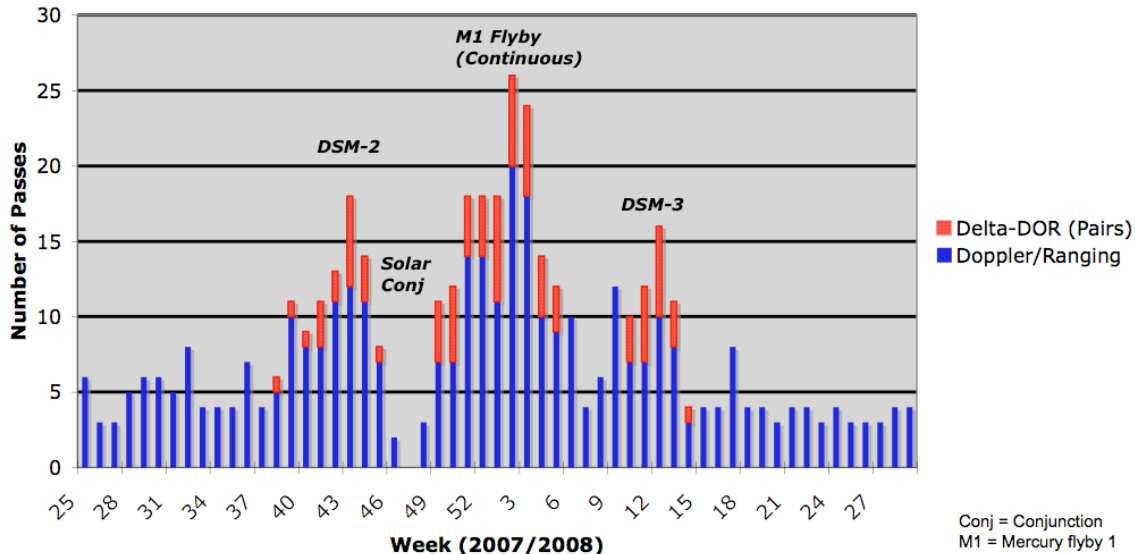


Figure 3. DSN Tracking Schedule Planned for MESSENGER around Mercury Flyby 1.

IV. MESSENGER Δ DOR Processing

Figure 3 also indicates special pairs of tracks associated with Δ DOR. The DSN Δ DOR tracking data type is formed by differencing two Very Long Baseline Interferometry (VLBI) measurements between a spacecraft tone signal and one or more nearby quasars. Since a VLBI measurement determines the spacecraft offset from the baseline between the two DSN antennas used in the measurement, the VLBI data provide a direct measurement of the spacecraft angular position relative to the baseline. During the Δ DOR tracking session, the two DSN antennas slew from the spacecraft to nearby quasars and return, taking a minimum of 10 minutes (min) of VLBI data from each source. The DSN currently performs a Δ DOR track by collecting VLBI data from a quasar, then both antennas slew to the nearby spacecraft, followed by a slew to a different quasar. The quasars are chosen so they are within about 10° of the DSN antenna pointing direction to the spacecraft. Normally, two complete quasar-to-spacecraft-to-quasar (Q1-S-Q2) sequences are performed during each Δ DOR track.

The individual VLBI measurements are subject to a variety of error sources including those due to media effects and various station-dependent parameters. Δ DOR provides cancellation of common error sources by forming the difference between the interleaved VLBI measurements of the spacecraft and nearby quasars. The difference ultimately results in a highly precise measurement of the angular offset between the spacecraft and the known location of the quasars used in the Δ DOR session. The accuracy of the spacecraft-quasar relative angular position is about 2 nanoradians, which is equivalent to 0.3 km at 1 astronomical unit (AU) in a direction normal to the spacecraft line-of-sight. Since single-station Doppler and ranging are line-of-sight measurements, the Δ DOR provides additional navigation information content in an “orthogonal” direction that is ideal for detecting and removing orbit determination errors in that direction. The addition of Δ DOR data provided a level of robustness and increased accuracy to the radiometric orbit determination at Mercury flyby 1, as well as both of the previous Venus flybys^{3,5}. As a result, Δ DOR data are planned for each of the remaining Mercury flybys and MOI.

In order to obtain a position measurement on the plane-of-sky, two nearly orthogonal baselines are used within the DSN: a roughly north-south baseline made up of antennas from the Goldstone, California, and Canberra, Australia, complexes, and a roughly east-west baseline made up of antennas from the Madrid, Spain, and Goldstone, California, complexes. When the Δ DOR data from north-south and east-west baselines are combined with Doppler and ranging in an orbit determination filter, the spacecraft position is very well determined in space. Figure 4 provides a breakdown of successful Δ DOR passes by baseline and also indicates passes that were either degraded (only one of two Q1-S-Q2 sequences completed) or failed (no successful sequence). Many of these failures arose from ground antenna slewing problems at specific DSN sites. Fortunately, enough Δ DOR passes were scheduled in advance such that the rate of failure was sufficiently low to avoid any serious impact on OD solutions. Δ DOR continues to make a significant contribution to accurate navigation of MESSENGER.

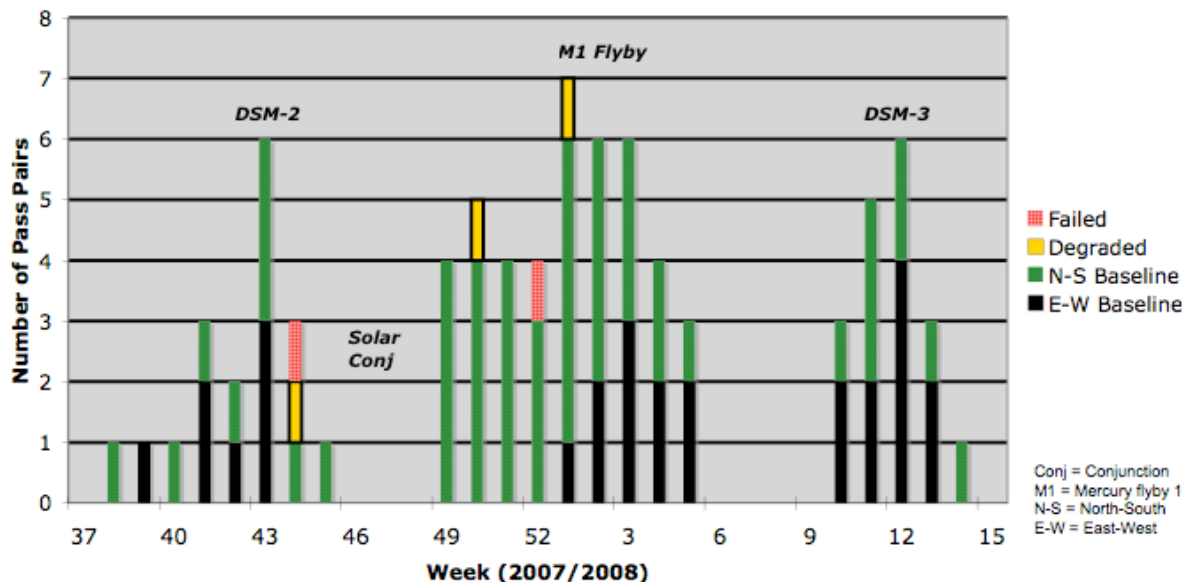


Figure 4. Resultant Δ DOR Tracks Associated with Mercury Flyby 1.

V. MESSENGER Optical Navigation Processing

The OpNav process for planetary flybys uses images of the target planet and background stars to determine the inertial pointing direction from the spacecraft to the planet. This gives a measure of the relative position and is a powerful measurement type to determine precisely the flyby conditions on approach and in a reconstruction. For MESSENGER, optical navigation, as a complement to the radiometric tracking, was planned for use in estimating the flyby conditions for the three Mercury flybys and the approach to MOI. Ideally, a single OpNav image would contain the planet and background stars. However, the MESSENGER cameras are science cameras made for mapping the bright surface of Mercury and not specifically designed for optical navigation, so individual images of the planet and of stars must be combined by the Navigation Team to form the OpNav measurement.

All OpNav images for MESSENGER are taken with the Mercury Dual Imaging System (MDIS). If an MDIS picture is over-exposed to image dimmer stars, then the planet is over-exposed and this causes stray light and image blooming problems that obscure fine details in the image. There are two cameras contained in the MDIS housing: one narrow-angle camera (NAC) with a 1.5° -square field of view (FOV), and one wide-angle camera (WAC) with a 10.5° -square FOV. Each camera has a 1024 by 1024 pixel charge-coupled device (CCD) in its respective focal plane for taking the picture. The NAC has a $25.5\text{-}\mu\text{rad/pixel}$ FOV, while the WAC has a $179\text{-}\mu\text{rad/pixel}$ FOV. The MDIS housing is mounted via a single-axis pivot to the spacecraft bus, so both NAC and WAC boresights are nominally co-aligned. MDIS cameras can be pointed by a combination of re-orientation of the spacecraft and moving the pivot.

Mercury flyby 1 afforded the first operational use of OpNav during the MESSENGER mission. Previous Earth and Venus flybys had not been suitable for operational support, largely because of the presence of an atmosphere that made accurate limb determination difficult, if not impossible. However, those previous opportunities did provide for calibration and tests of the imagers and the OpNav ground processing system, encompassing planning, scheduling, sequencing, downloading images, use of operational interfaces, and software enhancement³. The

culmination of these previous tests was a series of OpNav sequences for Mercury flyby 1, as described in Table 1. Each sequence includes eight images taken in rapid succession with the pivot angle of the MDIS fixed throughout the entire sequence. The entire sequence was completed within 15 min in each case. Of course, spacecraft attitude must be settled and recorded at the time each image is shuttered. The NAC is the primary imager for OpNav use, with the capability to image stars down to about 6.0 visual magnitude⁶. As indicated earlier, planets and stars are imaged separately and tied together via spacecraft attitude knowledge to determine inertial pointing direction. The WAC serves to provide an independent, low-resolution check on camera pointing.

Table 1. OpNav Sequence and Schedule.

Image #	Include Star*	Include Mercury	Camera	Exposure	DPU Binning	Filter	Note
1	Yes	No	NAC	10 sec	1x1	Clear	Star within 5-10 deg of planet and 20 pixels of boresight
2	Yes	No	NAC	10 sec	2x2	Clear	
3	Yes	No	NAC	10 sec	2x2	Clear	Offset 10 pixels to observe star relative to camera noise
4	No	Yes	NAC	auto	1x1	Clear	Planet within 20 pixels of boresight
5	No	Yes	NAC	auto	1x1	Clear	
6	Yes	Yes	WAC	10 sec	1x1	Clear	Same attitude and pivot angle; minimum time between images
7	Yes	Yes	WAC	auto	1x1	Clear	
8	Yes	Yes	WAC	auto	1x1	Clear	

*Star to Target:

OpNav #	Star ID (Tycho Catalog)	Visual Magn
1 and 5	1916-02156-1	3.7
2, 6 and 9	1359-02672-1	3.6
3 and 7	2457-02407-1	1.9
4 and 8	1920-02194-1	1.3

M1 = Mercury flyby 1
 CA = Closest Approach
 DPU = Data Processing Unit
 ID = Identification
 Magn = Magnitude

OpNav #	Epoch (UTC)	Rel to M1 CA [days]	Max download time after image acquisition [hrs]
1	09-Jan 11:00	-5.3	24
2	09-Jan 21:00	-4.9	24
3	10-Jan 09:00	-4.4	12
4	10-Jan 21:00	-3.9	12
5	11-Jan 09:00	-3.4	12
6	11-Jan 21:00	-2.9	6
7	12-Jan 09:00	-2.4	6
8	12-Jan 18:30	-2	2-3
9	13-Jan 06:30	-1.5	2-3

The OpNav approach campaign for Mercury flyby 1, as shown in Table 1, could not be initiated until all required camera pointings are a minimum of 40° from the Sun to avoid stray light problems and to observe SKI constraints on the spacecraft. For Mercury flyby 1, nine OpNav sequences were scheduled beginning 5.3 days before the encounter. Moreover, the internal center-finding algorithm had been upgraded after Venus flyby 2 to account for targets not entirely contained within an instrument FOV. Potential boresight offset biases were resolved and commanded pointing centered targets well enough that attitude updates in OpNav processing could be bypassed with a very fast turnaround of solutions, often within 30 min. Weightings of only 1 pixel were applied typically during the OpNav processing.

As indicated earlier, the main reason for employing OpNav at Mercury flyby 1 was to support design of a contingency maneuver (TCM-21) about 34 hours prior to closest approach, to raise or lower the final flyby altitude. This might have been required in the event of a large Mercury ephemeris error to avoid impacting the planet by adding excessive velocity changes or delta-V (ΔV) events after the flyby to return to a viable mission trajectory. The first six of nine OpNav sequences were used to narrow the maneuver design to three maneuver options, while the seventh and eighth sequences would lead to selection of a final maneuver candidate or a “no-go” decision on performing TCM-21. Due to TCM implementation constraints, the final OpNav sequence was performed too late to affect the decision on TCM-21, but it did support final confirmation and later trajectory reconstruction and characterization of the Mercury ephemeris error.

An example of one of the narrow-angle camera images taken as part of OpNav number three is shown in Fig. 5, where the crescent shape of the lit limb of Mercury is evident. The image as shown in Fig. 5 has been cropped over 50% to remove dark sky and focus on Mercury. Figure 6 shows the history of OpNav-based locations and uncertainties mapped into the Mercury B-plane. The earliest OpNav solutions tended to be biased to the right because the Mercury image on which they were based was a relatively narrow crescent, which acted to degrade the accuracy of the center-finding algorithm. Nevertheless, as more images were processed, OpNav solutions converged with concurrent radiometric OD solutions over time. The convergence of solutions away from the original aimpoint is the result of “solar sailing” to minimize errors primarily in the T-direction, and will be explained in a later section. This confirmed that the Mercury ephemeris from the DE405 planetary ephemerides, assumed for all MESSENGER radiometric solutions, was valid. In fact, the Mercury ephemeris was determined to be no more than 2 km from the Mercury ephemeris included in DE405. The post-fit OpNav residuals for the final estimation had respective means of 0.23 and 0.0029 for lines and pixels from all images, with standard deviations of 2.0 and 1.7 lines and pixels,

respectively. These residuals are slightly larger than the typical few tenths of a pixel that would be expected from a dedicated OpNav camera because the reduced sensitivity of MDIS required that star images and planet images be taken with different exposures in different directions. Special processing techniques for MESSENGER OpNavs allow the information from the star and planet images to be combined as they would be in a single image for other missions. In light of these restrictions, the MESSENGER OpNav worked extremely well during Mercury flyby 1.



Figure 5. Mercury Flyby Narrow-Angle Camera Image from OpNav Number Three.

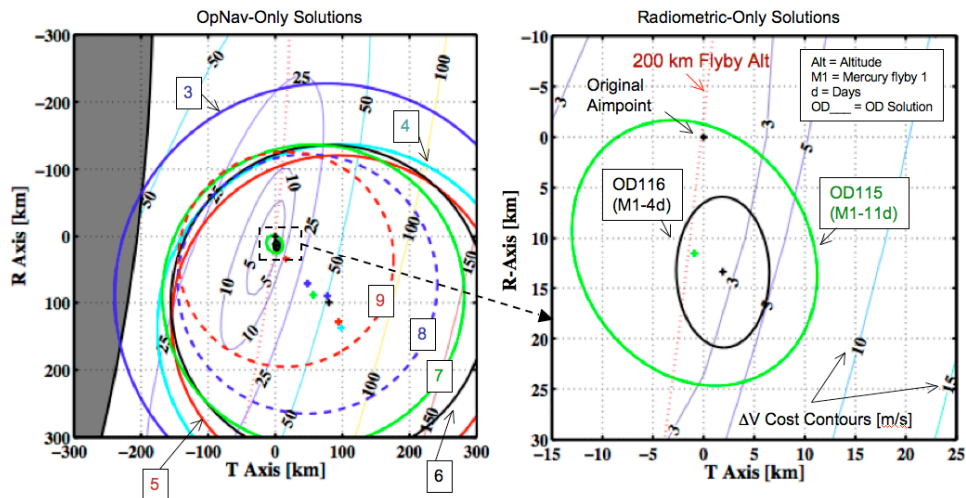


Figure 6. Mercury Flyby 1 OpNav Evolution and Convergence with Radiometric Solutions.

VI. MESSENGER Orbit Determination Results

A trajectory reconstruction was performed using the Doppler, ranging, and Δ DOR data available over the arc from Venus flyby 2 beyond Mercury flyby 1. The data started on 5 July 2007, 11:35, UTC (Greenwich Mean Time) after Venus flyby 2 and ended on 13 February 2008, 22:06 UTC, after Mercury flyby 1. The orbit determination filter arc includes two propulsive TCMs that were estimated and reconstructed as discussed below. The quality of the fit is demonstrated by the observation residuals, or the observed measurements minus the computed values based on the estimated parameters, which are presented in Fig. 7(a), 7(b), and 7(c). The different DSN antennas are indicated by different markers (letters) on the plot. The Doppler residual mean is +0.0002 millimeters per second (mm/s) or nearly zero with a standard deviation of 0.51 mm/s over the four-month data arc, which indicates a good fit to the Doppler tracking data. The low noise in the Doppler measurements is indicated by the small scatter on a pass-by-pass basis. The larger noise in the middle of the arc, in October and November 2007, is due to effects from solar plasma corresponding to a smaller SEP as MESSENGER was in the solar conjunction that occurred in November 2007.

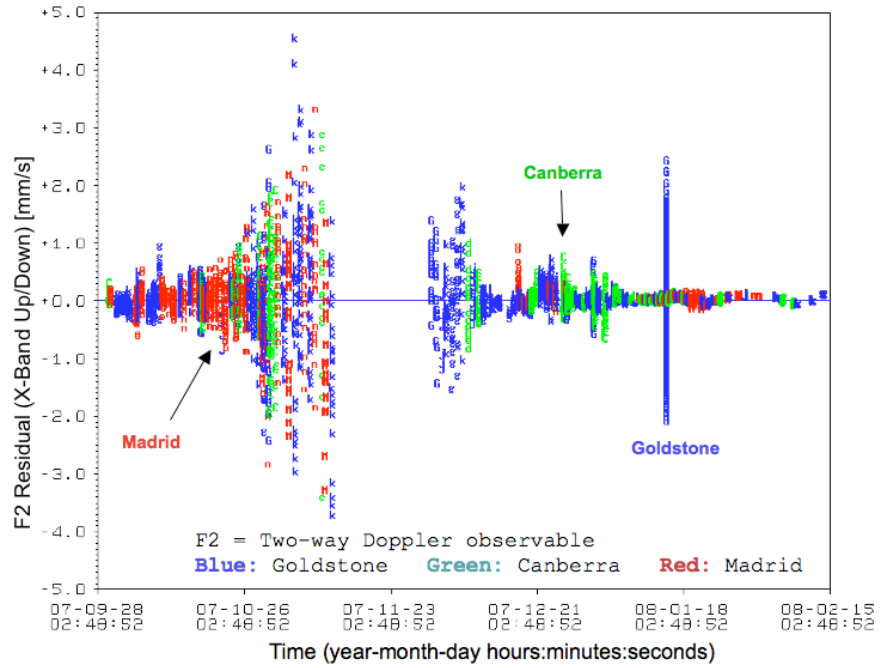


Figure 7(a). DSN 2-Way X-band Doppler (F2) Residuals for Reconstructed Trajectory from Venus Flyby 2 to Mercury Flyby 1.

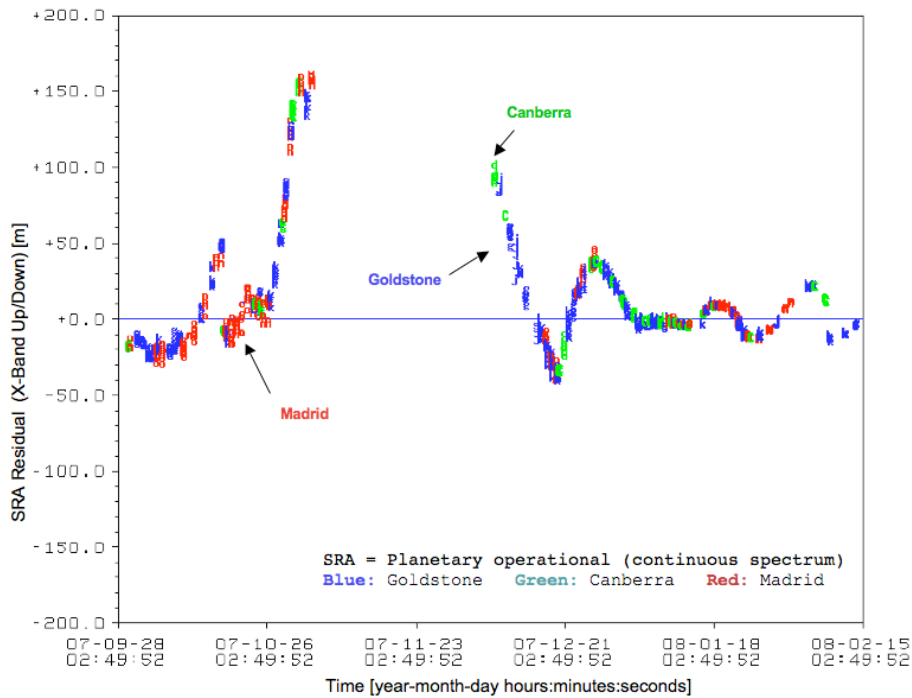


Figure 7(b). DSN 2-Way Sequential Ranging (SRA) Residuals for Reconstructed Trajectory from Venus Flyby 2 to Mercury Flyby 1.

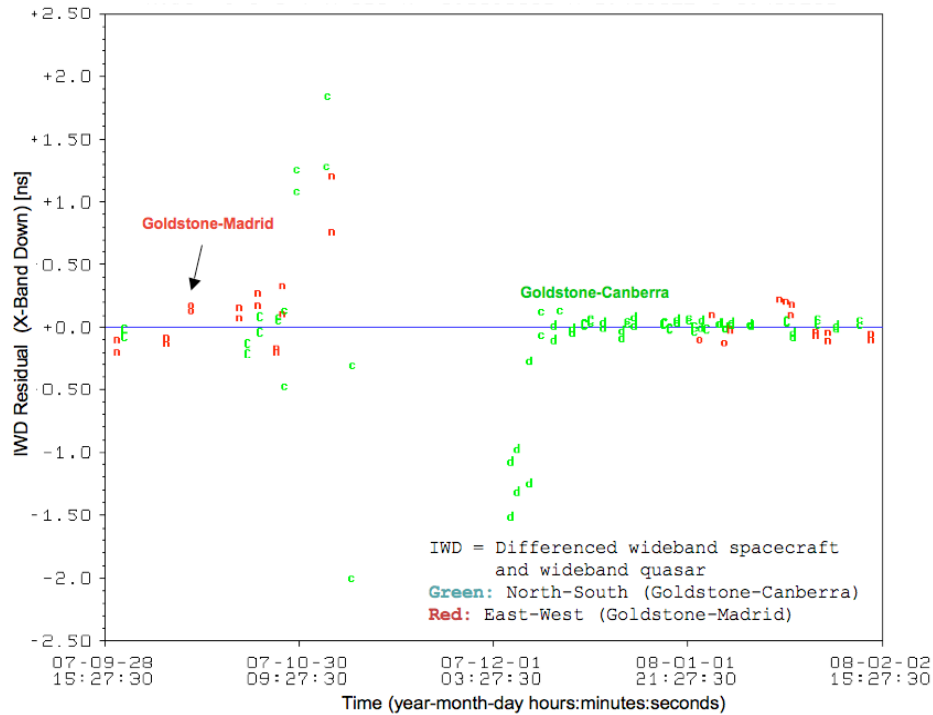


Figure 7(c). DSN Δ DOR Residuals for Reconstructed Trajectory from Venus Flyby 2 to Mercury Flyby 1.

There were a number of orbit determination challenges for the leg of the trajectory between Venus and Mercury. First, the observation geometries available at Mercury flyby 1 were not as favorable as those experienced at Venus flyby 2. The Earth-to-spacecraft range was more than 1.5 AU during much of the final approach to Mercury flyby 1, resulting in lower signal-to-noise and decreased precision in the ranging data. Adjustments to the relative weighting of the Doppler and ranging in the orbit determination filter minimized the impact this had on trajectory estimates. The encounter occurred about a month after a superior solar conjunction so tracking data was missing or degraded during the approach. Also, the Earth’s diurnal viewing direction was nearly orthogonal to the B-plane T-axis, so the enhanced accuracy in the altitude direction that occurred at Venus flyby 2 did not occur for Mercury flyby 1. The encounter occurred at low declination, so there was reduced overlap between the Madrid and Goldstone tracking stations, resulting in few Δ DOR east-west baselines during approach. However, overlap in tracking between Goldstone and Canberra was more abundant, so many north-south baselines of Δ DOR were in the schedule.

Next, there was the design of the final Mercury targeting maneuver just after emergence from the long solar conjunction with the expected large amount of solar-plasma-induced noise. Figure 8 shows the two-way Doppler and ranging residual means, noise, and weighting for the data arc from Venus flyby 2 to Mercury flyby 1. The “weights” plotted for the two-way Doppler are actually the *a priori* 1- σ assumed data noise used to calculate the weights via $W = 1/\sigma^2$. A stepped schedule of weights was applied for each degree of SEP smaller than 10° to account for solar plasma noise during the October–December superior solar conjunction. The weighting is generally chosen to be conservative compared with the actual noise. However, on the outbound side of the conjunction in particular, the plasma-induced noise was considerably less than expected. This was fortunate, because the design for TCM-19 (to clean up DSM-2) occurred the day after the conjunction formally ended when the SEP was again greater than 3° , so that almost all of the radiometric data after DSM-2 used for the design of TCM-19 was entirely within the conjunction at SEP of less than 3° .

The weightings for ranging are more conservative than Doppler, since ranging typically is subject to more variation over a long data span, both from incompletely modeled dynamics and from the large delays that can be induced by deficiencies in the media calibrations and solar plasma. Although the noise for individual passes is usually quite good, typically to just a few meters, the ranging variations over longer times can be much larger. The ranging variations in this span are quite reasonable and are smaller than 10 m around closest approach.

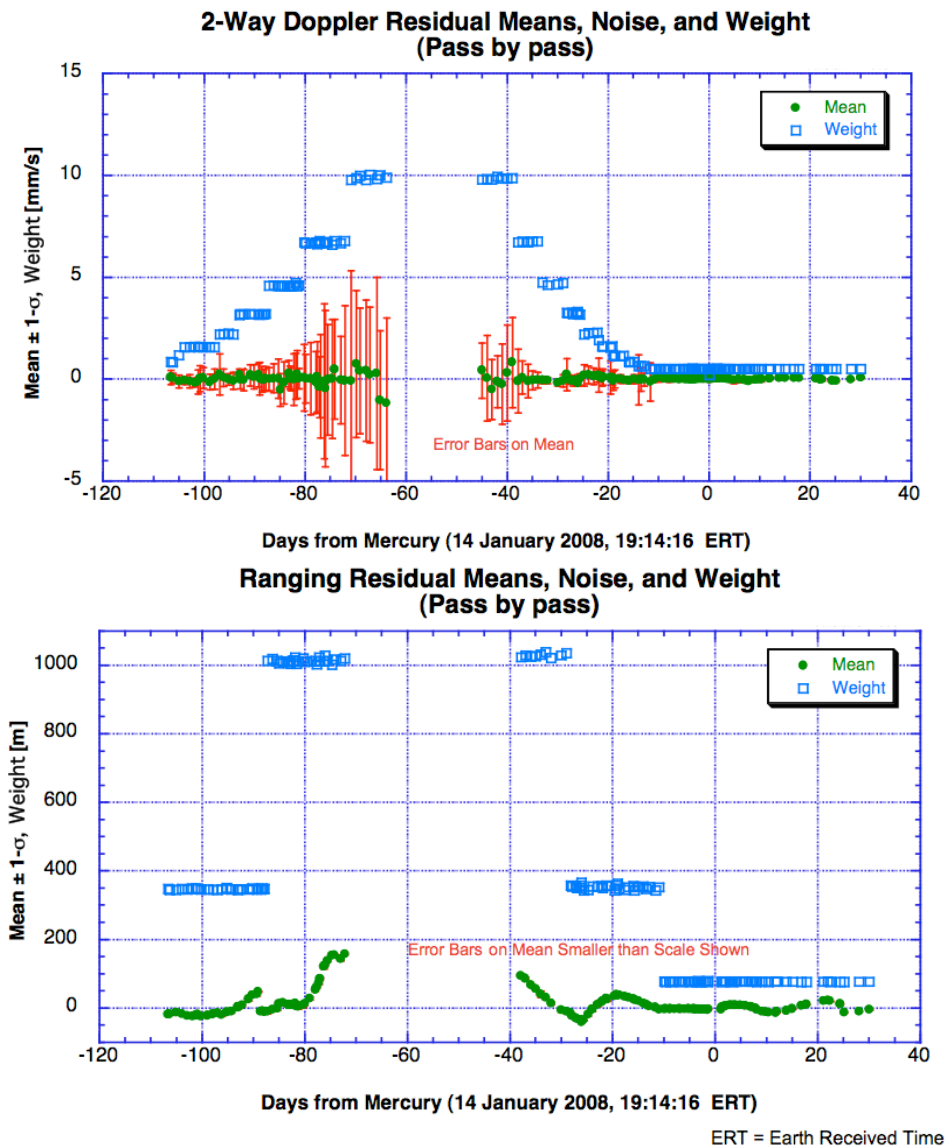


Figure 8. Two-Way Doppler and Ranging Residual Means, 1- σ Noise, and Weighting for the Data Arc from Venus Flyby 2 to Mercury Flyby 1.

Finally, the flyby also had the closest heliocentric range to date for the spacecraft, which put more emphasis on the solar pressure modeling. Solar pressure modeling was also impacted by the many attitude changes needed for passive angular momentum control and Earth pointing associated with the low SEP. Finally, solar panel offsets of up to 70° off the Sun put new stress on correct modeling of the attitude and solar pressure. Moreover, there was an unknown acceleration on the spacecraft around the time of the spacecraft perihelion on 1 September 2007 at a distance from the Sun of 0.33 AU. Attempts to model this acceleration through perihelion were unsatisfactory, and ultimately the decision was made to split the data arc into two segments, with the first span beginning on 5 July 2007 and ending 30 September 2007, one month after the spacecraft made its closest approach to the Sun. The second arc began at this point and ended 13 February 2008, about one month after Mercury flyby 1. It was found that the solutions obtained with this shorter arc were more stable and provided a better estimate of the spacecraft B-plane intercept.

Figure 9 shows the evolution of the orbit determination solutions in the B-plane. Execution of TCM-19 at around 26 days prior to the flyby introduced considerable noise into the solution, but this was largely removed via

additional post-maneuver tracking, and errors diminished significantly over the following week. A comparison of the B-R solution in this plot with the Δ DOR schedule shows the utility of the Δ DOR data obtained after exiting the solar conjunction. The B-R direction is not as well determined by Doppler and ranging data alone. The inclusion of the Δ DOR data starting at around 40 days prior to flyby enabled the solution to converge to within a few kilometers of the final reconstructed estimate. As mentioned once before, a targeting offset in B-R relative to the ideal aimpoint was accepted to accommodate “solar sailing” that served to minimize errors primarily in the T-direction. Targeting strategy will be explained further in a later section.

Prior to the second Venus flyby, a covariance analysis had been performed to predict navigation performance for the trajectory leg between Venus and Mercury. This study was done using the expected DSN tracking data schedule and operational models employed by the Navigation Team, but before detailed knowledge of the dynamics acting on the spacecraft and operational tracking data schedule were known. The trajectory errors are presented in terms of the size of the semi-major and semi-minor axes of the error ellipse in the B-plane, along with the in-track component normal to the B-plane (in the S-direction).

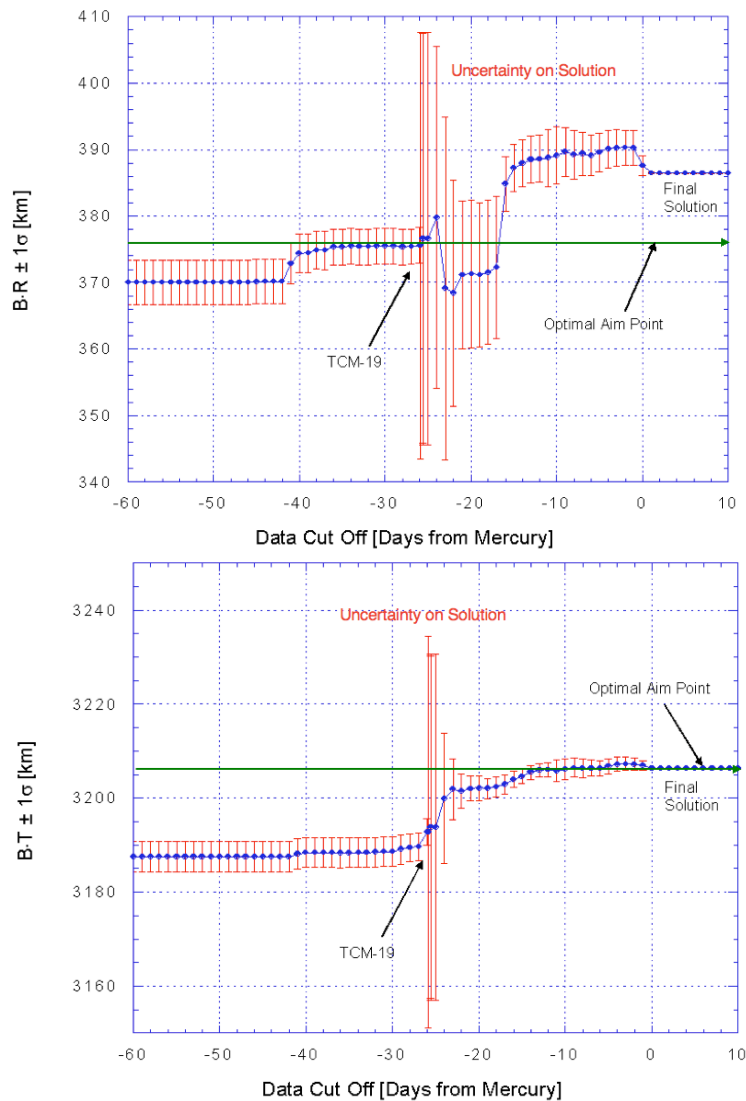


Figure 9. B-R and B-T Uncertainties on Approach to Mercury Flyby 1.

VII. MESSENGER Maneuver Analysis

As mentioned previously, two nominal DSMs were planned, one before and one after the Mercury flyby 1, to keep the spacecraft on course over subsequent flybys and the eventual orbit phase about Mercury. Several other TCM opportunities have been accommodated in the schedule to address cleanup of possible execution errors and operational contingencies, as shown in Table 2.

A. Maneuver Accuracy and Capabilities

The accuracy of maneuvers is characterized by the parameters shown in Table 3, which specifies execution errors in both magnitude and direction for various thruster modes and ΔV ranges, as certified by MESSENGER Guidance and Control (G&C) lead engineer, Dan O'Shaughnessy. Thruster sets are identified in Fig. 10 and are shown relative to spacecraft axes and nominal spacecraft-to-Sun orientation. The larger maneuvers, such as DSMs, are performed mainly in thruster mode 3 with the large velocity adjust (LVA) thruster, which uses a bipropellant (bi-prop) mixture of fuel and oxidizer to achieve ΔV in excess of 20 m/s. The sets of smaller thrusters use a monopropellant (mono-prop), with the next highest range of ΔV achieved using the C thruster set supplied from the primary fuel tank. Use of this particular set of thrusters is identified as thruster mode 2, capable of achieving ΔV up to 30 m/s. Remaining thruster sets are identified as mode 1 and use monopropellant supplied from an auxiliary fuel tank, which is refilled as part of the sequence performed for larger velocity corrections. Mode-1 thrusters are typically used only for smaller velocity corrections during approach maneuvers prior to each planetary flyby.

Table 2. Maneuver Opportunities Associated with Mercury Flyby 1.

Maneuver	Epoch	Purpose	Used?
TCM-17	18-Jul-07 (V2+43d)	Recover from extreme targeting error left over from Venus flyby 2.	N
DSM-2 (TCM-18)	17-Oct-07 (M1-89d)	Supply $\Delta V \sim 227$ m/s to achieve Mercury flyby 1 on 14 January 2008.	Y
DSM-2C1	23-Oct-07 (DSM-2+6d)	As backup to DSM-2, supply $\Delta V \sim 221$ m/s to achieve Mercury flyby 1 on 14 January 2008.	N
DSM-2C2	30-Oct-07 (DSM-2+13d)	Final contingency to complete a partially executed DSM-2 within acceptable Sun keep-in pointing constraints ($<12^\circ$).	N
TCM-19	19-Dec-07 (M1-26d)	Clean-up residual Mercury flyby 1 targeting error left over from DSM-2.	Y
TCM-19C1	26-Dec-07 (M1-19d)	Contingency for TCM-19, primarily to address potential delay in OD solution coming out of solar conjunction.	N
TCM-19C2	31-Dec-07 (M1-14d)	Final contingency to complete TCM-19.	N
TCM-20	10-Jan-08 (M1-4d)	Clean-up residual Mercury flyby 1 targeting error left over from TCM-19.	N
TCM-21	13-Jan-08 (M1-34h)	Avoid Mercury impact or excessive ΔV cost arising from large Mercury ephemeris error as revealed by OpNav approach campaign.	N
TCM-22	5-Feb-08 (M1+22d)	Recover from extreme targeting error left over from Mercury flyby 1.	N
DSM-3 (TCM-23)	19-Mar-08 (M1+65d)	Supply $\Delta V \sim 72$ m/s to achieve Mercury flyby 2 on 6 October 2008; provide initial test of "turn-while-burn" mode to be employed at MOI.	Y
DSM-3C1	24-Mar-08 (DSM-3+5d)	As backup to DSM-3, supply $\Delta V \sim 71$ m/s to achieve Mercury flyby 2 on 6 October 2008.	N
DSM-3C2	27-Mar-08 (DSM-3+8d)	Final contingency to complete a partially executed DSM-3 within acceptable Sun keep-in pointing constraints ($<12^\circ$).	N

V2 = Venus flyby 2 M1 = Mercury flyby 1 d = days Y = Yes N = No

Table 3. Maneuver Opportunities Associated with Mercury Flyby 1.

ΔV Magnitude	0.005 – 3 m/s	0.005 – 3 m/s	3 – 8 m/s	3 – 8 m/s	0.5 – 30 m/s	20 – 300 m/s
Thrusters	Mode 1 A/B/P	Mode 1 S	Mode 1 A/B/P	Mode 1 S	Mode 2 C mono-prop	Mode 3 LVA bi-prop
Proportional Magnitude	1.00%	1.00%	3.50%	3.50%	0.60%	0.11%
Fixed Magnitude	4.3 mm/s	4.3 mm/s	4.3 mm/s	4.3 mm/s	33.6 mm/s	63.8 mm/s
Proportional Pointing	31.3 mrad	100 mrad	31.3 mrad	100 mrad	5.0 mrad	2.0 mrad
Fixed Pointing	3.9 mm/s	3.9 mm/s	3.9 mm/s	3.9 mm/s	17.6 mm/s	18.7 mm/s

Per-axis pointing errors are $1/\sqrt{2}$ times the values above; Mode 1 is usually on the auxiliary tank.

Typically the orientation of the sunshade relative to the Sun imposes operational constraints on usage of various thrusters. A SKI limit of 9° nominally, and 12° at a maximum, limits the use of lateral thrusters (A, B, C and LVA) to off-Sun thrusting directions in the range of 81° to 99° nominally (or 78° to 102° at a maximum). If ΔV is needed at other angles, this necessitates a radial implementation using the P or S thrusters alone or a vector decomposition into radial and lateral components, as indicated in Fig. 11, with an attendant ΔV penalty. The latter is inherently impractical for DSMs or larger TCMs.

B. Targeting Considerations

Targeting errors, in turn, arise from the cumulative effects of both orbit determination errors and maneuver execution errors as the mission unfolds. Targeting errors at Mercury flyby 1 have potentially severe consequences, not only in terms of impacting the planet, but for increasing mission ΔV cost to return to an optimal trajectory, as shown in Fig. 12, with an expanded view on the right showing closer details. Note that, while missing the target at lower altitudes has consequences in terms of ΔV cost and impacting Mercury, the mission cost contours are steeper at higher altitudes and can also have severe or mission-ending consequences. The contours reflect global mission cruise ΔV usage sensitivity to flyby errors, while achieving subsequent flyby conditions in order to arrive at Mercury in March 2011 and meet orbit insertion requirements. The axes indicate the change in B-T and B-R from the minimum-total- ΔV (through MOI) trajectory. The contours allow for trajectory re-optimization beyond Mercury flyby 1 to minimize ΔV costs as much as possible. The penalty for larger misses is more severe in the B-T direction than along B-R.

C. Effect of Trajectory Correction Maneuvers

DSM-2 occurred before the conjunction leading into the first Mercury encounter. In addition to DSM-2, only one other

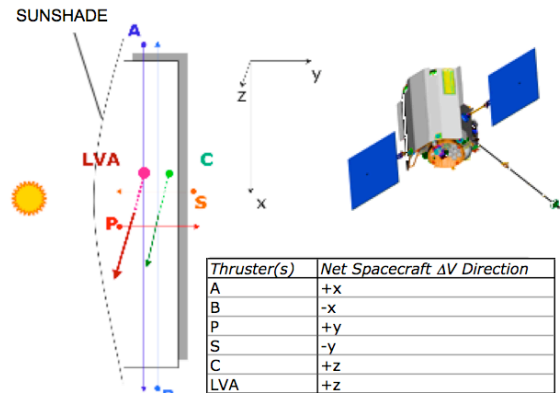


Figure 10. MESSENGER Thruster Orientation.

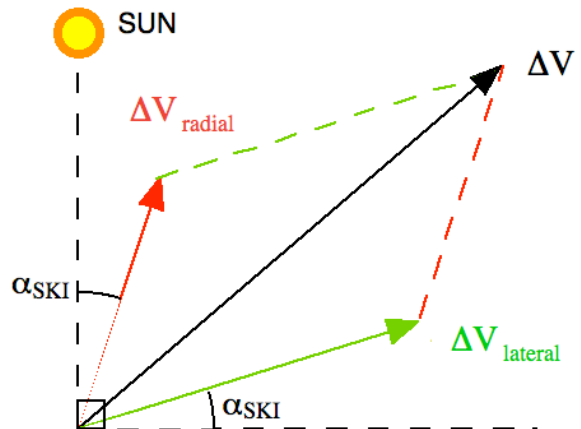


Figure 11. Maneuver Decomposition to Avoid SKI Violation.

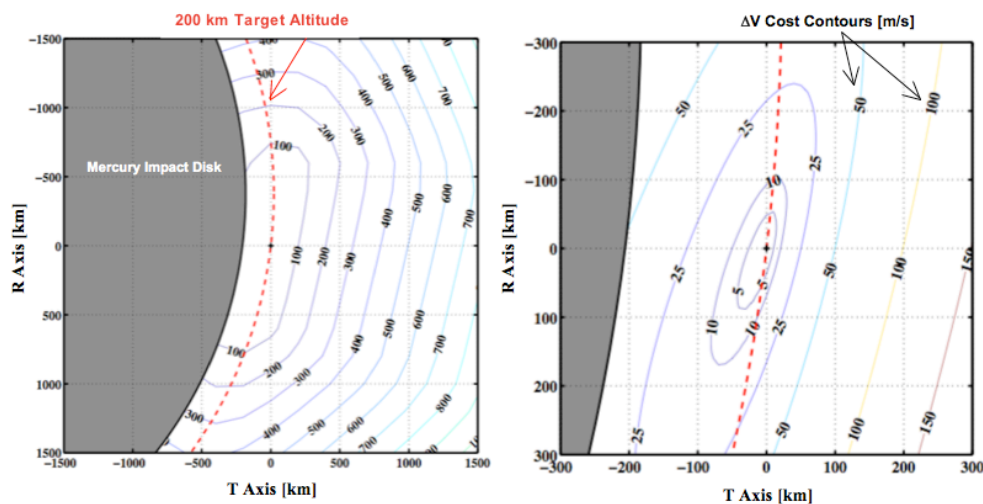


Figure 12. MESSENGER Mercury Flyby 1 B-Plane and Mission Cost Contours.

TCM was required to correct errors in targeting to the aimpoint for Mercury flyby 1, as indicated in Table 2. Table 4 indicates the Δv for each maneuver design and the reconstruction based on subsequent OD solutions. DSM-3, which occurred after Mercury flyby 1 as a prerequisite to achieve the next Mercury encounter, is also described here.

Table 4. Design and Reconstruction of TCMs before and after Mercury Flyby 1.

TCM [DSM]	Execution Date (Relative Days)	Coord Frame	Mvr Seg	Thr Mode	Final Maneuver Design			Final Nav Reconstruction			Reconstructed Execution Error	
					Mag [m/s]	RA [deg]	Dec [deg]	Mag [m/s]	RA [deg]	Dec [deg]	Mag [m/s]	Ptg [deg]
18 [2]	17-Oct-07 (M1-89d)	EME2000	A	3	226.017	113.2	23.4	225.992	113.4	23.2	-0.025 (-0.01%, -0.1 σ)	0.22 (1.9 σ)
			B	1	1.421	113.2	23.4	1.421	110.3	23.1	-0.0006 (-0.04%, -0.04 σ)	2.64 (1.5 σ)
19	19-Dec-07 (M1-26d)	EME2000	A	1	1.104	357.1	38.4	1.104	357.4	38.4	-0.0006 (-0.06%, -0.05 σ)	0.22 (0.1 σ)
23 [3]	19-Mar-08 (M1+65d)	EMO2000*	A	1	0.159	321.3	8.4	0.159	321.4	8.3	0.000 (-0.05%, -0.02 σ)	0.10 (0.04 σ)
			B†	3	69.617	321.3	8.4	69.611	321.3	8.4	-0.0058 (-0.01%, -0.06 σ)	0.05 (0.4 σ)
			C	2	2.470	322.0	4.5	2.471	322.0	4.5	0.0005 (0.02%, 0.01 σ)	0.05 (0.09 σ)

* Ecliptic reference used here to fully emulate MOI design in support of test of turn-while-burn mode.

† RA and Dec shown are initial directions; assumed RA and Dec turn rates of 0.00748 and -0.0431 deg/s, respectively, during burn.

Coord = Coordinate Mvr = Maneuver Thr = Thruster Mag = Δv Magnitude RA = Right Ascension Dec = Declination Ptg = Pointing

M1 = Mercury flyby 1 d = days

DSM-2 was a critical maneuver required to achieve the Mercury flyby 1. DSMs typically consist of a mode-1 settling burn to achieve optimal placement of the LVA oxidizer and fuel, followed by a mode-3 main burn on the LVA thrusters with auxiliary tank refill and a final mode 1 or 2 trim maneuver. For DSM-2, the initial settling burn was small enough to be discounted as a separate burn and is included as part of the LVA component, as indicated in Table 4. A long superior solar conjunction (SEP < 3°) commenced around October 27 and ended on December 12. Ideally, DSM-2, or one of two backup maneuvers targeted to a re-optimized aimpoint for Mercury flyby 1, would be completed prior to solar conjunction. During the conjunction period, contact with the spacecraft would be problematic at best, and the ability of operations to deal with spacecraft anomalies would be severely limited. Fortunately, DSM-2 was executed on 17 October 2007. The effect of DSM-2 on the B-plane targeting at Mercury flyby 1 is depicted in Fig. 13.

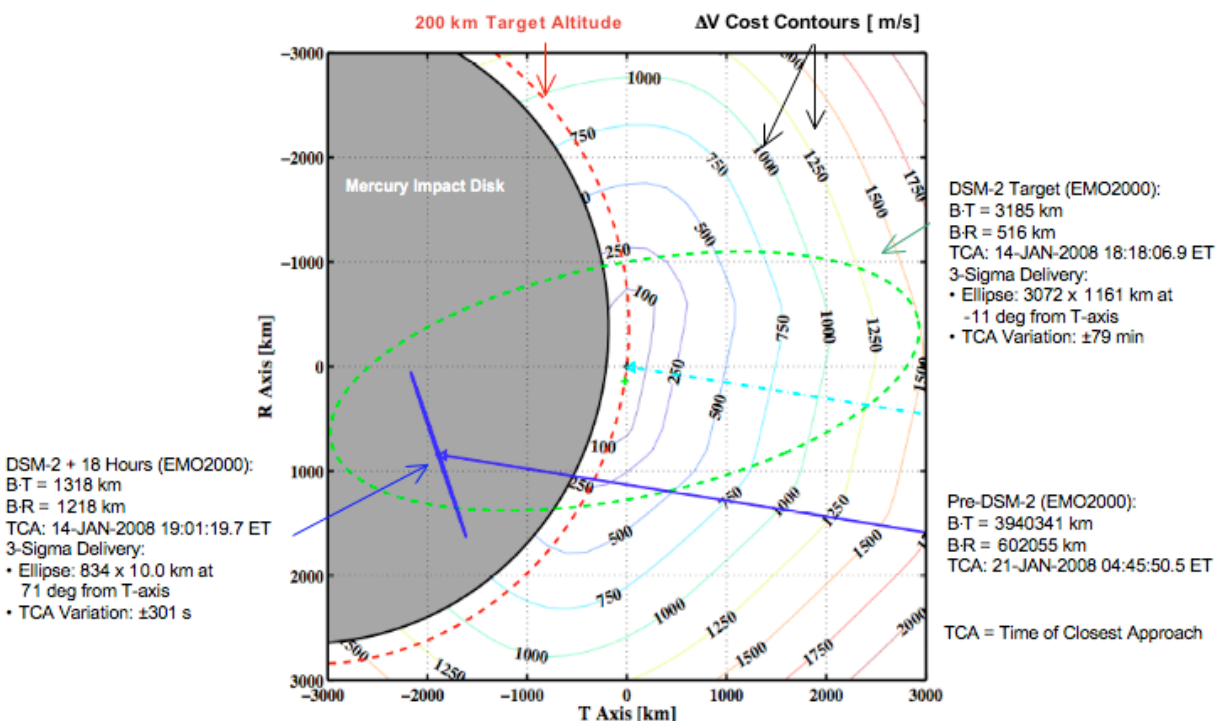


Figure 13. Mercury Flyby 1 B-Plane Target Shift Effected by DSM-2.

A final contingency maneuver for DSM-2 was scheduled as late as October 30 to complete a partial DSM-2 burn or a large execution error that might have resulted from poor engine performance or another spacecraft system anomaly. Although there was evidence of a relatively large pointing error (2 σ), which left the spacecraft on an

impact trajectory with Mercury, it was deemed less risky to wait until TCM-19, after the solar conjunction, to perform further trajectory corrections. This cleanup maneuver was scheduled after reliable tracking was re-acquired post-conjunction, so the approach timeline was more compressed than that at Venus flyby 2. At this point, there was a little less than one month from closest approach, with five additional opportunities prior to 14 January 2008 to move the spacecraft away from Mercury. TCM-19 was determined, after adjusting TCA to produce a design for a lateral maneuver, to require about 1.1 m/s on 19 December 2007. Also, the targeted closest approach time was shifted from 14 January 2008, 18:18:07 ephemeris time (ET) to 19:05:47 ET to establish a lateral orientation for the TCM-19 design. Note that ET is a time scale that excludes discontinuities associated with leap seconds, and is currently offset from UTC by about +65 s.

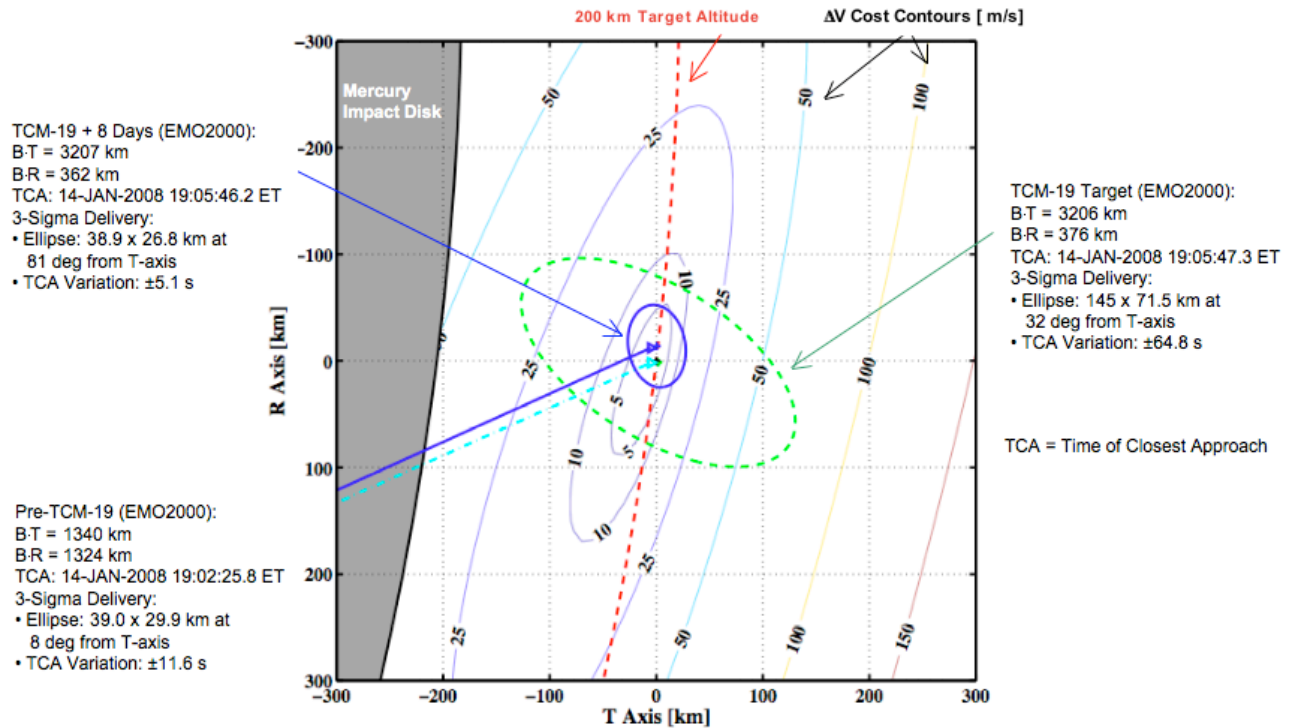


Figure 14. Mercury Flyby 1 B-Plane Target Shift Effected by TCM-19.

The nominal TCM-19 on 19 December 2008 was executed with a high degree of accuracy, as indicated in Table 4. Much of this performance was due to characterization of previous TCMs performed in mode 1 with A and B thrusters, which enabled systematic errors to be determined and accelerometer biases applied to the maneuver implementation. As shown in Fig. 14, execution of TCM-19 moved the B-plane intercept point away from Mercury and very close to the flyby target. Successful completion of TCM-19 allowed for cancellation of contingency maneuvers identified as TCM-19C1 and TCM-19C2.

After additional tracking data were processed over the following two weeks, OD solutions decreased in uncertainty but tended to drift slightly farther away from the target point into a region lying between mission cost contours of 3 and 5 m/s, albeit with some probability of exceeding 10 m/s, as shown in Fig. 15. A small corrective maneuver of 3-4 centimeters per second (cm/s), based on use of radial (P) or lateral (A/B) thrusters appeared to be needed to move as close to the target as possible and minimize subsequent mission ΔV penalty. Although TCM-19 had been executed very accurately, there was concern about accurate execution of such a small maneuver. Moreover, the operations team was focused on preparations for the upcoming Mercury flyby 1 and was concerned about minimizing workload and risk in light of the perception of only a marginal benefit in terms of ΔV savings.

Fortunately, an alternate approach was uncovered that avoided making a trade between risk and ΔV usage. This approach involved making adjustments to spacecraft attitude and solar panel tilt angles, affecting the solar radiation pressure cross-section of the spacecraft, while meeting power and thermal constraints vital to the survival of MESSENGER near perihelion. Adjustments, akin to “solar sailing,” were applied to the predicted attitude profile over the period of two weeks that remained prior to the Mercury flyby 1. As indicated in Fig. 15, the overall effect was to move the OD solution closer to a flyby altitude of 200 km, consistent with the selected target B·T. Note that

the mission ΔV cost contours tend to be aligned in the direction of B-R. Thus, although B-R was not corrected, and in fact was slightly exacerbated by the “solar sailing”, the impact on mission ΔV was minimized. This result was acceptable as an alternative to performing TCM-20, so that this maneuver, scheduled for 10 January 2004 or four days prior to closest approach, could be cancelled.

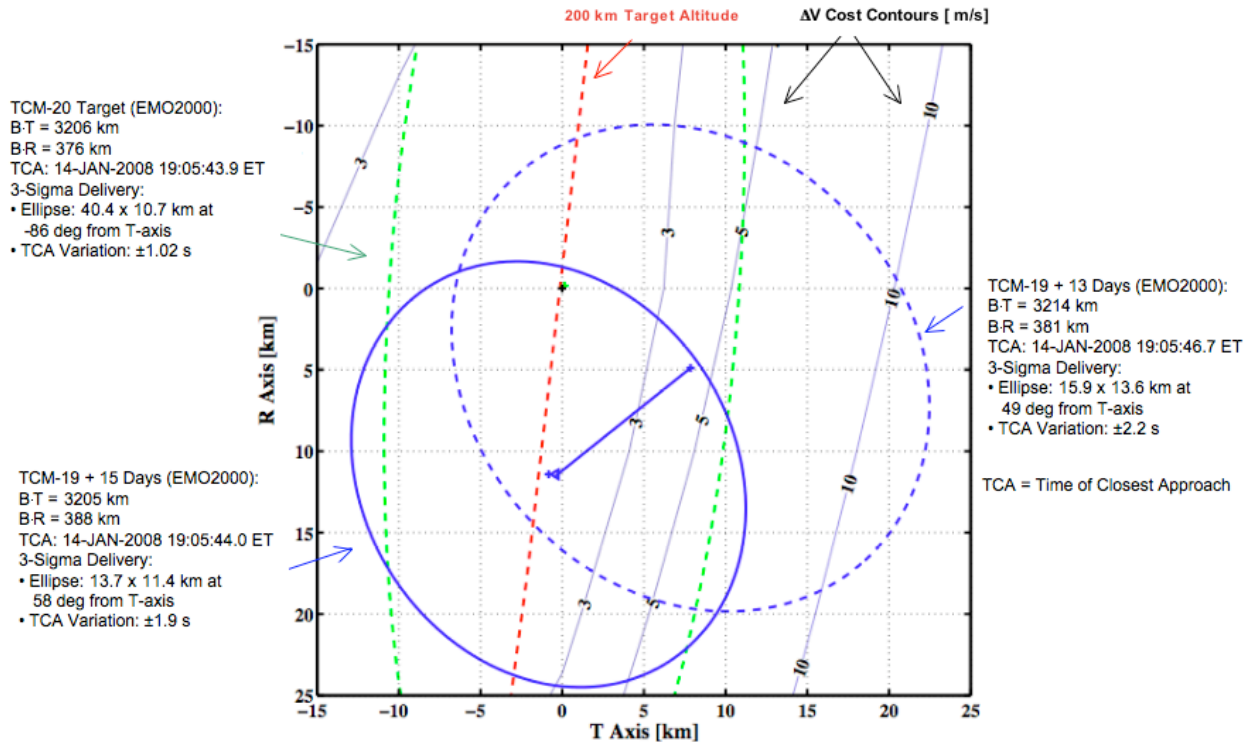


Figure 15. Mercury Flyby 1 B-Plane Target Shift Effectuated by “Solar Sailing” in Lieu of TCM-20.

As noted previously, the remaining maneuver opportunity was TCM-21, scheduled at 34 hours prior to closest approach. TCM-21 was a radial design using either P thrusters to move away from Mercury or less accurate S thrusters to move closer, as might be required to avoid more excessive mission ΔV cost. No spacecraft turns would be needed, only a ΔV magnitude and thruster selection. Because the aforementioned “solar sailing” was effective and OpNav solutions converged with radiometric OD solutions, indicating an insignificant Mercury ephemeris error, TCM-21 was not required. The final, reconstructed flyby location is about 10 km below the aimpoint for Mercury flyby 1.

After the flyby, there was a provision for executing TCM-22 on 5 February 2008, to set the stage for DSM-3. Fortunately, owing to the relatively insignificant flyby error, trajectory re-optimization allowed for a nominal DSM-3 on 19 March 2008, with a direction well within SKI limits, so TCM-22 was cancelled. DSM-3 was designed at around 80 m/s, much smaller than previous DSMs. Because of the small size, in part, DSM-3 afforded an opportunity to test implementation features of MOI. In particular, turning the spacecraft at a constant rate in both right ascension (RA) and declination (Dec) during the LVA burn will be required at MOI to inject MESSENGER most efficiently into orbit about Mercury. Therefore, this turn-while-burn mode was practiced at DSM-3, utilizing turn rates in the Earth Mean Orbital Plane of the J2000 (EMO2000) coordinate frame of the same magnitude that would be required for MOI. In this case, the small settling burn was treated as a separate component, since no turning occurred prior to the LVA portion of the maneuver. Also, the final maneuver component was performed on C thrusters in this case to avoid draining the auxiliary tank and to keep the center of mass stable for momentum management. Although DSM-3 is less than one tenth the magnitude of MOI, the turn-while-burn implementation provided useful insights into the performance of the spacecraft, and the small turn angle (about 3.9°) engendered only an additional 0.2 m/s or so penalty in DSM-3 execution when compared with doing no turn at all.

Based on the resultant ΔV , DSM-3 performance for the main burn (component B) was significantly improved over DSM-2 (component A), as indicated in Table 4. In the aftermath of DSM-3, as indicated in Fig. 16, pending further OD updates, it was determined that a trajectory correction on the order of 10 cm/s might be sufficient about a

month prior to the second Mercury encounter to achieve the desired targeting conditions. Moreover, as a result of the close collaboration between the Navigation Team and G&C engineers, it has been possible to manipulate spacecraft attitude and solar panel articulation so that a successful Mercury flyby 2 is likely without any further TCMs. The success or shortfall of this strategy will be reported in a future paper.

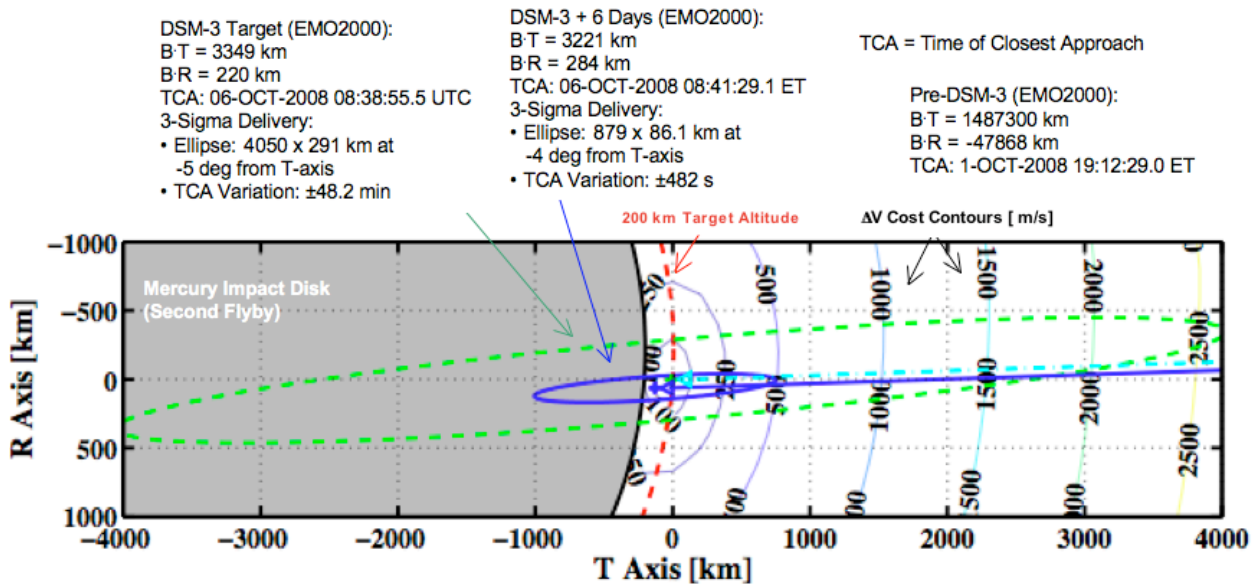


Figure 16. Mercury Flyby 2 B-Plane Target Shift Effected by DSM-3.

VIII. Determination of Mercury Gravitational Field and Planetary Ephemeris

In order to obtain a good reconstruction of the trajectory through the flyby, it was necessary to construct an engineering model of the Mercury gravitational field. Figure 17 shows the large two-way Doppler residual signature remaining, as a function of Earth Received Time (ERT), when *a priori* values of J_2 and C_{22} were used but none of the gravity harmonics was estimated⁷. All other harmonics were assumed to be zero. Data begin with 1-sec measurements after the end of Earth occultation. 1-min data measurements begin at about 19:30 ERT, and 10-min

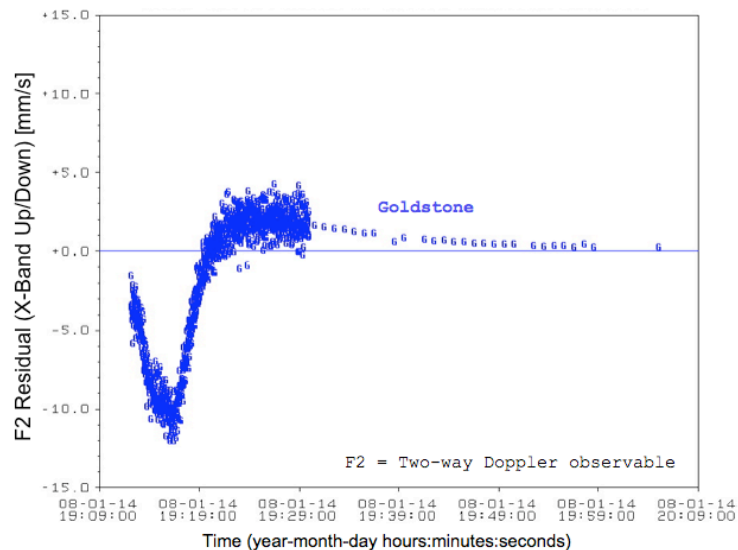


Figure 17. Two-way Doppler Residuals (mm/s) Versus ERT (UTC) in the Vicinity of Mercury Closest Approach.

measurements resume at about 20:00. Periapasis is at 19:14:16 ERT. Figure 18 shows a significant improvement in the size of the signature when J_2 , C_{22} , and S_{22} are estimated, but there is still an interesting structure left over in the residuals.

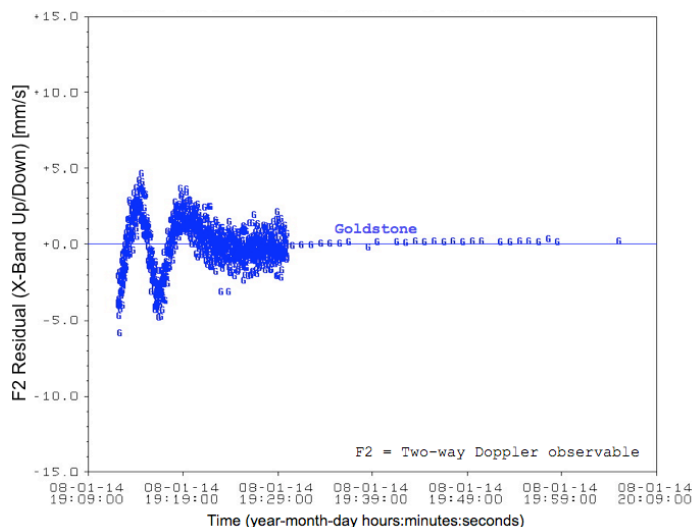


Figure 18. Two-way Doppler Residuals (mm/s) Versus ERT (UTC) in the Vicinity of Mercury Closest Approach When Estimating J_2 and C_{22} .

An engineering model of the Mercury planetary ephemeris was generated during the course of the post-flyby trajectory reconstruction, obtained by solving for the heliocentric position of Mercury in the orbit determination process. The differences between the Mercury ephemeris given by DE405 and that estimated after the flyby is given in Table 5.

Table 5. Heliocentric Differences in Mercury and Earth Positions at the Time of Closest Approach, in the Earth Mean Equator of J2000 (EME2000) Frame.

	ΔX (km)	ΔY (km)	ΔZ (km)
Earth	0	0.2	-0.4
Mercury	0.1	1.6	-0.5

IX. Lessons Learned and Future Plans

The planetary flybys and flight operations thus far on MESSENGER have provided valuable calibration and insight for performing the remainder of the mission. The lessons learned will be incorporated into the remaining Mercury encounters.

Since reconstruction demonstrated that Mercury ephemeris errors were tiny, any lingering concerns about Mercury planetary ephemeris error were put to rest. Such confirmation of the Mercury ephemeris reduces the criticality of OpNavs at subsequent Mercury encounters. Therefore, all remaining opportunities will be used only to test the OpNav system and complete adjustments needed for landmark tracking prior to the Mercury orbit phase. OpNav operations during Mercury flyby 1 revealed minor issues to be resolved on subsequent flybys. The residual bias in the image processing evident in the earliest Mercury flyby 1 images needs to be resolved. Adjustments to the OpNav schedule and the auto-exposure strategy will be employed at Mercury flyby 2.

As an aside, the most definitive OpNav solutions based on the latest images occurred too late to support the decision for TCM-21 (last contingency maneuver). Use of the work-around previously described, based on a simplified radial (S/P) thruster design, might be considered under similar circumstances for future missions. However, because of the demonstrated accuracy of the Mercury ephemeris, it is unlikely that such a late maneuver will be required again on the MESSENGER mission. Hence, future contingency approach maneuvers can be

scheduled several days in advance of the flyby merely to provide backup opportunities to previous TCM or targeting correction activities.

Most approach TCMs can still be performed most accurately with lateral (A/B) thrusters, as long as the closest approach time at the upcoming encounter is allowed to shift by several minutes to accommodate this directional constraint. G&C was able to remove systematic error at TCM-19 by applying a biased pointing offset that produced an excellent outcome leading to cancellation of TCM-20. The $\sim 2\sigma$ pointing error for DSM-2 compels further characterization, but the outcome from DSM-3 seems promising. Further characterization of DSMs should culminate in further improvements in future DSMs and MOI. Furthermore, “solar sailing” shows promise as an alternative means of trajectory correction, provided that the required correction is relatively small or can be planned far enough in advance to be achievable within constraints imposed by power and thermal subsystems. More extensive Δ DOR has proven once again to be a major contributor to OD accuracy. A specific Δ DOR schedule is recommended for the remainder of cruise phase, including a total of 43 measurements for future legs between encounters. This provides for accurate reconstruction of large DSMs on each leg, using tracks before and after a DSM, and supports design of a DSM cleanup, which occurs typically five weeks after the DSM. The schedule includes six measurements, each requiring overlapping DSN pass coverage from Goldstone and Canberra or Madrid during three weeks prior to DSM and six more in the three weeks following the maneuver. More Δ DOR passes are recommended to support accurate design of the next to last normal maneuver before each encounter, intended to clean up any trajectory errors remaining, or accrued, since the preceding DSM. This entails nine measurements during the period from five to two weeks before the TCM. Additionally, 18 measurements are requested to support events during the last six weeks before each encounter, including design and reconstruction of contingency or scheduled maneuvers remaining before the encounter. Finally, four measurements are recommended in the two weeks subsequent to an encounter for reconstruction and support of a post-encounter cleanup maneuver, if needed. As always, Δ DORs should be scheduled about 50-50% on each baseline whenever possible. Use of this technique is planned on approach to Mercury flyby 2.

Events associated with the perihelion on 1 September 2007 complicated OD processing and tended to reduce observability of other events and distort the mapped B-plane solution. Possible causes include SRP modeling error, boil-off of high-temperature volatiles, and/or solar-panel angle errors. Nevertheless, based on correlation with momentum wheel and other data enhancements on observed anomalies provided by G&C, the Navigation Team was able to reconstruct the spacecraft trajectory up through and including Mercury flyby 1 with an acceptable degree of accuracy. Although such effects are expected to diminish as the mission progresses, OD around perihelion is still a moderate concern, and further efforts at improved characterization of spacecraft behavior over these periods will continue. Experience gained in accounting for these effects during this phase should pay off later in the mission. Moreover, shortening up fit arcs used for OD solutions remains as a fallback in many cases when modeling problems prove too difficult to resolve with limited time and resources.

X. Conclusion

The first Mercury encounter culminated in a relatively accurate delivery. Reconstruction placed the spacecraft 10.3 km from the targeted B-plane aimpoint and 2.7 s from targeted time of closest approach. The post-flyby ΔV costs of not achieving the precise B-plane target are estimated to be no more than 2 m/s, a modest increment considering that only 1.1 m/s was used at TCM-19 to perform the only propulsive maneuver on final approach to Mercury flyby 1. Moreover, the Mercury planetary ephemeris was essentially confirmed via OpNav solutions on approach and the reconstruction afterwards, and processes to be employed for refinement of an engineering model of Mercury’s gravity field were initially tested. Performance of TCMs continued to improve steadily, with no major anomalies. Execution of DSM-3 provided a notable performance improvement over DSM-2 and offered an initial rehearsal opportunity for operational modes to be employed for MOI, from which much was learned. Manipulation of spacecraft attitude and solar panel articulation (“solar sailing”) was demonstrated as a substitute for the final nominal TCM during approach. In light of the challenges faced with regard to the preceding long solar conjunction, as well as the first operational use of OpNav and provision for quickly responding to a potential Mercury ephemeris error, the first Mercury encounter by the MESSENGER spacecraft was deemed a great success.

Acknowledgments

The MESSENGER Navigation Team acknowledges the able and professional support of NASA’s Deep Space Network Critical Events Planning Team, the MESSENGER Network Operations Project Engineer (NOPE), and the

Radio Metric Data Conditioning Team (RMDC) for acquiring the radiometric tracking data that make this work possible. The navigation team also wishes to thank Dr. James Border of the Jet Propulsion Laboratory for his support in providing processed data from Δ DOR passes, James K. Miller, formerly of KinetX, Inc., for development and application of OpNav software, Dr. Robin Vaughan of JHU/APL for extensive help to implement the OpNav images in the MESSENGER spacecraft sequences, and Daniel O'Shaughnessy of JHU/APL for his efforts to improve maneuver accuracy and development of "solar sailing" as an alternative to certain TCMs. The MESSENGER mission is supported by the NASA Discovery Program Office under contracts to the Carnegie Institution of Washington (CIW) and JHU/APL. This work was carried out by the Space Navigation and Flight Dynamics Practice of KinetX, Inc., under a subcontract with CIW.

References

- ¹McAdams, J. V., Dunham, D. W., Farquhar, R. W., Taylor, A. H. and Williams, B. G., "Trajectory Design and Maneuver Strategy for the MESSENGER Mission to Mercury," *J. Spacecraft Rockets*, 43 (5), pp. 1054-1064, 2006.
- ²Williams, B. G., Taylor, A. H., Carranza, E., Miller, J. K., Stanbridge, D. R., Page, B. R., Cotter, D., Efron, L., Farquhar, R. W., McAdams, J. V. and Dunham, D. W., "Early Navigation Results for NASA's MESSENGER Mission to Mercury," *Adv. Astronaut. Sci.*, 120 (Part II), pp. 1233-1250, 2005.
- ³Williams, K. E., Taylor, A. H., Page, B. R., Miller, J. K., Smith, J., Wolff, P., Stanbridge, D., Williams, B. G. and McAdams, J. V., "Navigation for the Second Venus Flyby of the MESSENGER Mission to Mercury," *Adv. Astronaut. Sci.*, 130 (Part II), pp. 1113-1132, 2008.
- ⁴Thornton, C. L., and Border, J. S., "Radiometric Tracking Techniques for Deep-Space Navigation," *Deep-Space Communications and Navigation Series – Monograph 1*, Wiley-Interscience, pp. 47-58, 2003.
- ⁵Taylor, A. H., Carranza, E., Miller, J.K., Stanbridge, D. R., Page, B. R., Smith, J., Wolff, P., Williams, B. G., Efron, L., Farquhar, R. W., McAdams, J. V., and Dunham, D. W., "Earth to Venus-1 Navigation Results for NASA's MESSENGER Mission to Mercury," *Adv. Astronaut. Sci.*, 127 (Part I), pp. 1081-1100, 2007.
- ⁶Høg, E., Fabricius, C., Makarov, V. et al., "The Tycho-2 Catalogue of the 2.5 Million Brightest Stars," *Astron. Astrophys.*, 355, pp. L27-L30, 2000, web site <http://www.astro.ku.dk/~erik/Tycho-2/>.
- ⁷Anderson, J. D., Colombo, G., Esposito, P., Lau, E. and Trager, G., "The Mass, Gravity Field, and Ephemeris of Mercury," *Icarus*, 71, 337-349, 1987.